Methods 140–141 (2018) 52–61

Contents lists available at ScienceDirect

Methods

journal homepage: www.elsevier.com/locate/ymeth

Scanning fluorescence correlation spectroscopy comes full circle

German Gunther, David M. Jameson, Joao Aguilar, Susana A. Sánchez *

Laboratorio de Cinética y Fotoquímica, Facultad de Ciencias Químicas y Farmacéuticas, Universidad de Chile, Santiago, Chile
Department of Cell and Molecular Biology, John A. Burns School of Medicine, University of Hawaii, Honolulu, HI, USA
Universidad de Concepción, Facultad de Ciencias Químicas, Departamento de Polímeros, Concepción, Chile

ARTICLE INFO

Article history:
Received 31 October 2017
Received in revised form 23 January 2018
Accepted 30 January 2018
Available online 7 February 2018

Keywords:
FCS
Circular scanning FCS

ABSTRACT

In this article, we review the application of fluorescence correlation spectroscopy (FCS) methods to studies on live cells. We begin with a brief overview of the theory underlying FCS, highlighting the type of information obtainable. We then focus on circular scanning FCS. Specifically, we discuss instrumentation and data analysis and offer some considerations regarding sample preparation. Two examples from the literature are discussed in detail. First, we show how this method, coupled with the photon counting histogram analysis, can provide information on yeast ribosomal structures in live cells. The combination of scanning FCS with dual channel detection in the study of lipid domains in live cells is also illustrated.

Contents

* Corresponding author at: Universidad de Concepción, Facultad de Ciencias Químicas, Departamento de Polímeros, Concepción, Chile.
E-mail address: susanchez@udec.cl (S.A. Sánchez).

https://doi.org/10.1016/j.ymeth.2018.01.023
1046-2023/

1. From point to circular scanning FCS

1.1. Nano-historical overview

Fluctuation methods have been utilized for more than a century, dating back to the theoretical work of Albert Einstein in 1905 [1] and Marian Ritter von Smolan Smoluchowski (1906) [2] on Brownian diffusion and the experimental studies by Theodore Svedberg on colloids in 1911 [3]. Application of fluctuation analysis to light scattering began in the 1960s, and in the early 1970s Elson, Magde and Webb developed fluorescence correlation spectroscopy (FCS) and used it to study binding reactions and chemical kinetics [4,5]. Independently, in 1974, Ehrenberg and Rigler developed the method to study rotational diffusion of macromolecules [6]. In 1990, Denk and Webb [7] demonstrated microscopy based on two-photon excitation and in 1995 Berland, So and Gratton put the two technologies together, namely two-photon excitation microscopy and Fluctuation Correlation Spectroscopy (FCS), and demonstrated the potential of this methodology for intracellular measurements [8]. Elliott Elson, one of the pioneers of FCS, has written a series of historical overviews of the method well worth the attention of anyone with a sustaining interest in FCS [9–11].

Scanning FCS refers to an extension of FCS where the focal volume is moved relative to the sample to measure correlation functions in both space and time. Scanning FCS was introduced in 1976 by Weissman [12], who used a circular rotating sample cell (keeping the excitation volume fixed) to expose several statistically independent volumes to the illumination beam providing, in addition, a way of separating the desired fluctuation from the noise. In 1986 Petersen [13] published FCS measurements in 3T3-cells using a custom designed linear translating stage having a position detector allowing control of the sample position with a precision of ~20 nm.

1.2. Fluorescence correlation Spectroscopy: fluctuations in one spot

The basic principles of FCS have been discussed in many publications [11,14]. Initially, microscopy and FCS were realized using a single point of excitation and observation as illustrated in Fig. 1 [14]. Some instruments use standard confocal pinhole methods to achieve the very small observation volume while others use two-photon principles which are intrinsically confocal [15]. In point FCS, the small illumination volume is kept immobile and the signal fluctuations detected will arise from the instrumental noise and from the stochastic Brownian motion of molecules moving randomly in and out of the illumination volume as a function of time. As the figure indicates, if the concentration of fluorophores is sufficiently low, then fluctuations in the signal are evident. Analysis of these fluctuations provides information on the motility (diffusion coefficients), concentration (number of particles) and association state (molecular brightness) of the particles responsible of the fluctuations observed. To extract this information, data can be analyzed by using the Autocorrelation Function (ACF) or the Photon Counting Histogram (PCH).

Consider the data stream depicted in Fig. 2. The average fluorescence intensity in the data stream is termed $\langle F(t)\rangle$, while the variation of any point from the average is termed $\delta F(t)$. To calculate the autocorrelation function, $G(\tau)$, the intensity at some time, t, is multiplied by the intensity at a later time, $t + \tau$, as illustrated in Fig. 2a. The average of this product, carried out for many values of τ, is then divided by the square of the average fluorescence intensity to generate the value $G(\tau)$.

$$G(\tau) = \frac{< \delta F(t) \times \delta F(t+\tau) >}{< F(t) >^2} \quad (1)$$

By carrying out this calculation over many τ values, an entire autocorrelation curve is constructed, as shown in Fig. 2b. Two parameters can be recovered from the ACF analysis: the diffusion coefficient (D_{coef}) and the average number of particles in the observation volume ($\bar{N}$) given by the inverse of G (0) and multiplied by a constant (γ) that depends on the illumination profile.

For PCH analysis [16,17] the probability of detecting photons per sampling time is calculated from the histogram of the detected photons, comparing the theoretical with the experimental distribution. The occupation number of particles freely diffusing in

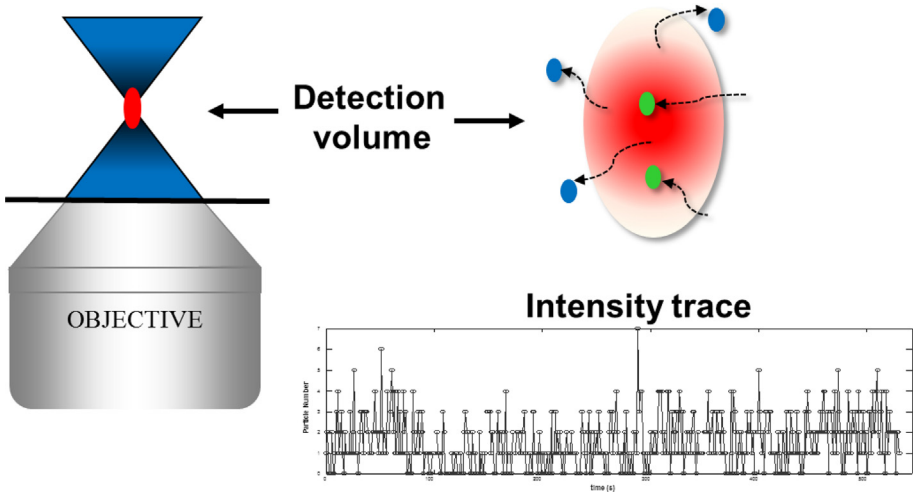

Fig. 1. Fluctuations are measured in a small volume (femtoliter range). The small illumination volume is generated either by the use of pinholes or directly by using two-photon excitation.

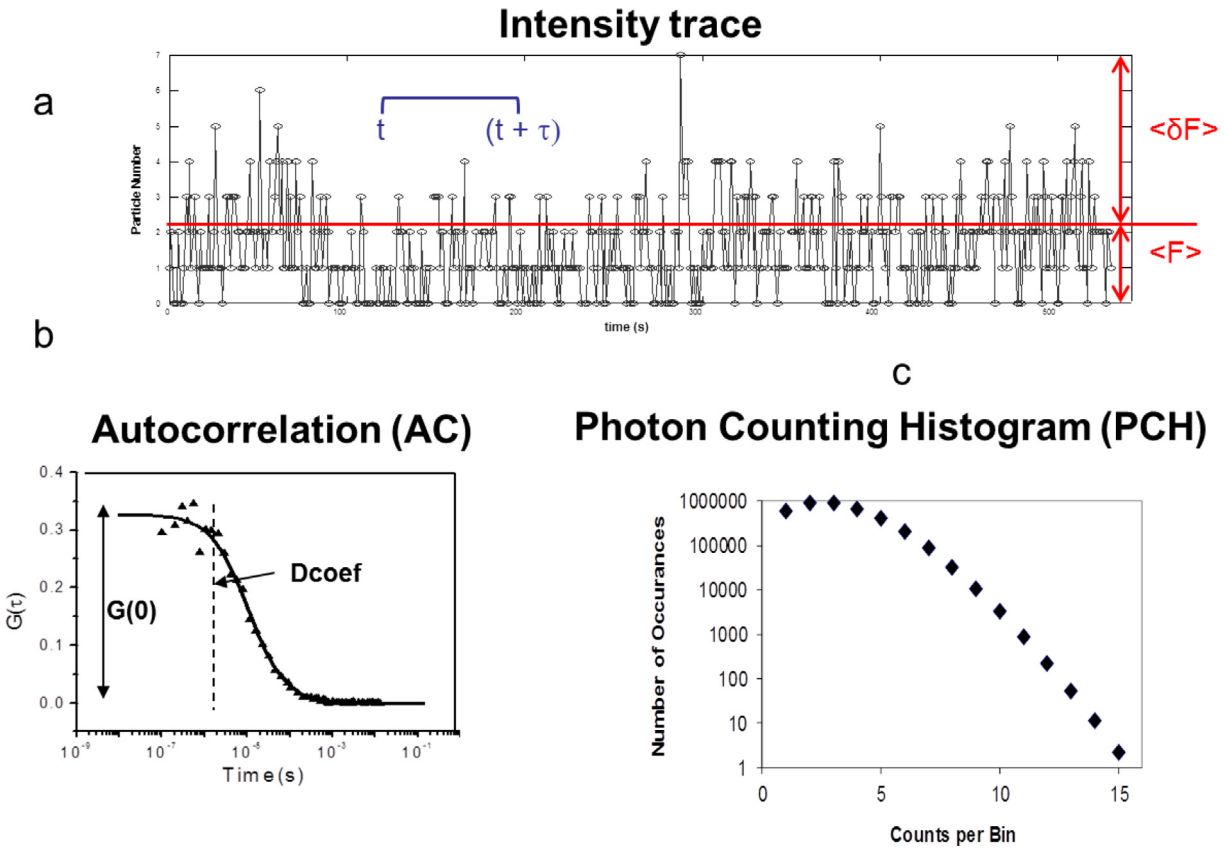

Fig. 2. Data analysis in FCS. (a) Intensity trace showing the parameters used for the autocorrelation (AC) (b) and photon counting histogram (PCH) analysis.

and out a small excitation volume is described by a Poisson distribution (Fig. 2c). The analysis is performed by determining the deviation of the measured distribution of photons from the expected Poisson distribution due to the diffusion of molecules in an inhomogeneous excitation profile and the statistics of the photon counting detector. Two parameters characterize the photon distribution: the number of molecules in the observation volume ($\bar{N}$) and the molecular brightness (β), which is defined as the average number of detected photons per molecule per second (Fig. 2c).

1.3. Circular scanning FCS: increasing spatial resolution

FCS is a technique with high temporal resolution where the illumination volume is kept immobile. In order to explore a larger area using this technique, one needs to perform either individual measurements of point FCS in several locations or to increase the spatial resolution by scanning several points in a period of time short enough to observe the molecule of interest. In 1994 Koppel [18] used a commercially available confocal system to perform linear scanning for collecting concentration fluctuation data on fluorescently labeled DNA molecules in solution and colloidal gold-tagged lipids in a planar bilayer. In 1996 Berland [19] using galvomotor-driven scanning mirrors to circularly move the laser beam, introduced the application of two-photon excitation to scanning FCS and demonstrated the capability of measuring particle number concentrations in solution and the application of the technique to study protein aggregation in solution. In 2005, Skinner et al. [20] scanning the sample in a circular fashion, introduced position-sensitive SFCS (PSFCS), where correlations are calculated as a function of lag time and phase allowing evaluation of the correlations for every position along the scanned trajectory.

Several improvements and applications have been realized after these initial descriptions [21]. In particular circular scanning FCS has been used *in vitro* and *in vivo* to study association of proteins [22–24], and lipid membranes [25–27]. The earliest implementations of the scanning approach utilized fixed illumination and a translating sample stage [12,13]. Present-day scanning, though, is almost always accomplished by keeping the sample stationary while scanning the laser beam.

Depending on the scanning trajectory different spatial and temporal resolution can be reached and the techniques received the name of the scanning mode (Fig. 3); the more commonly used are Circular scanning where scanning is performed following a circular orbit [19] and linear scanning (lineal trajectory) [28]. If the scanning is performed in a raster mode the spatial resolution increases but the temporal range of information decreases. A maximal spatial resolution is reached when using raster scanning and creating an image that can be fully analyzed by Raster Image Correlation spectroscopy, RICS [29].

The use of circular and line scanning allows high temporal resolution, while still providing spatial information. In both type of scanning the intensity fluctuations are acquired at many different locations to create a spatial map of diffusion coefficients and concentrations. The circular FCS method is particularly useful in cases in which precise localization of the excitation beam in a particular target area is difficult - for example, a membrane. By scanning across the membrane, one is sure to have the beam traverse the target area, and if a circular scan is utilized, the beam will cross the membrane twice during each scan. The data stream can then be presented as a "carpet" that renders evident which data are associated with particular regions. One advantage of the circular and line scanning modes of the laser beam on a membrane is that

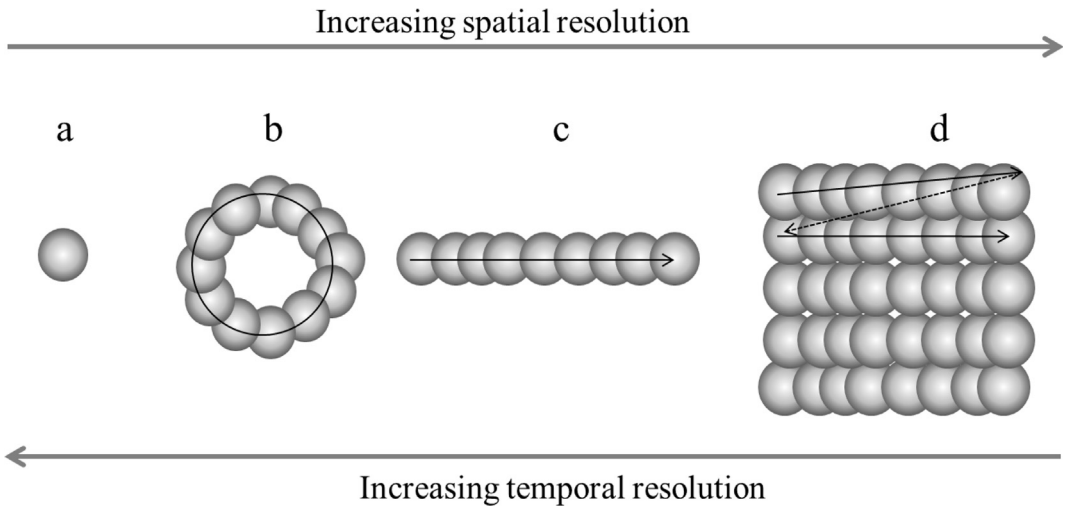

Fig. 3. Increasing spatial resolution for FCS by multiple sampling. (a) Illumination volume (point spread function, PSF) obtained by the use of pinhole or by two photon excitation. This volume remains immobile in traditional FCS acquisition. To increase spatial resolution the illumination volume can be move in a circular (b) or linear (c) trajectory. Maximal spatial resolution is obtained in raster scanning (d).

artifacts due to photobleaching of the dye is minimized. Such photobleaching can be severe for single point FCS on membranes [30] since membrane proteins diffuse relatively slowly [23].

Compared to single-point FCS, scanning FCS (circular and line) has several advantages when the system under observation moves or changes shape during the measurements. For example with live cells and giant liposomes, in csFCS the extra slow fluctuation due to sample movement can be corrected during the analysis [30]. A potential disadvantage of the csFCS approach is the possibility of missing some fast molecules, which diffuse away during the scan. However, as we will discuss later, in cell work this issue is not a major problem. If the measurements are done inside a cell one can measure movements and concentrations of molecules in the cytosol, in the membrane, inside particular organelles etc [22]. It is important to mention that decreasing temporal resolution to study cells is not a disadvantage. Molecules inside cells move approximately 4 times slower than in solution, for instance, GFP with a molecular weight of ~27 kD, in solution shows a D_{coef} = 87 $\mu m^2/s$, while in the cytosol free GFP has a D_{coef} = 23 $\mu m^2/s$ [23]. When proteins are inserted in the membrane, the mobility is restricted even more and the values for D_{coef} decrease to 1–0.1 $\mu m^2/s$ [23,31].

For circular scan microscopy, and also line and, raster-scan, the adjacent volumes along the orbit are sampled very quickly but the same volume in two consecutive orbits is sampled at a much slower rate. Thus, the registered data contains information from adjacent sampled volumes (spatial correlation) and from the same sampled volume but taken at different orbits (temporal information). We will consider here the temporal correlation analysis only, since spatial correlations are specifically measured by other techniques such as pair correlation [32] and raster image correlation (RICS) [29], and are not the focus of this article.

1.4. Circular scanning FCS: how slow should the laser scan

As mentioned earlier, inside cells molecules move approximately 4–5 times slower than in solution. An important question is how slow can we sample a location in order to detect the fluorescence fluctuation of molecules inside the cells? The average time (t) required by the molecules to move across the detection volume (diffusion time) depends on its D_{coef} (a term including considerations of the molecule's shape and size and also the temperature and viscosity of the medium) and on the specific optical setup (including W_0, the width of the point spread function (PSF) [31]). For one-photon excitation, the diffusion time is given by:

$$t = w_0^2/4D_{coef} \quad (2)$$

The average value of w_0 (PSF width) is ~0.35 μm. Using the Eq. (2) and reported diffusion coefficients, we can calculate the diffusion times for different compounds. For Rhodamine 110 (D_{coef} = 430 $\mu m^2/s$) [33], EGFP in solution (D_{coef} = 87 $\mu m^2/s$) [23] and EGFP in the cell cytosol (D_{coef} = 23 $\mu m^2/s$) [23] their respective diffusion times will be 0.0712, 0.352 and 1.3 ms. Therefore repetition rates of 0.5–1 ms for the circular orbit will be sufficient to detect EGFP diffusing inside the cells, although faster diffusing molecules will be missed. Inside cells, the D_{coef} reported range from 4 to 20 $\mu m^2/s$ and in the cell membrane the values range from 0.5 to 0.04 [23,34].

1.5. Circular scanning FCS: data acquisition and analysis

Fig. 3 shows a diagram to explain data acquisition and analysis in circular scanning FCS. The diagram shows an example in which a 1 ms orbit is used to scan a desired region. The scanner is moving clockwise and FCS data are acquired at six locations designated 1–6. The data are organized in a x-y representation (carpet) where the x-axis display the locations and the y-axis contains the temporal information of the fluctuation at each location. The time taken by the laser to complete the orbit and come back to the first point corresponds to the $\Delta time$ between the fluctuations (in Fig. 4, $\Delta time$ = 1 ms). Thus, each location has an intensity trace (with repetition time = 1 ms) that can be analyzed as point FCS data by either AC or PCH analysis (Fig. 2). In this example FCS data are taken at six locations around the orbit without any overlap of the PSF. Depending on the study, overlapping sampling is not really needed but adds the possibility of spatial correlation analysis of the data [32].

1.6. Circular scanning FCS (csFCS): data analysis [19,26,29,35]

The mathematical expression for the temporal correlation in FCS is given by

$$G_s(\tau) = S(\tau) \times G(\tau) \quad (2)$$

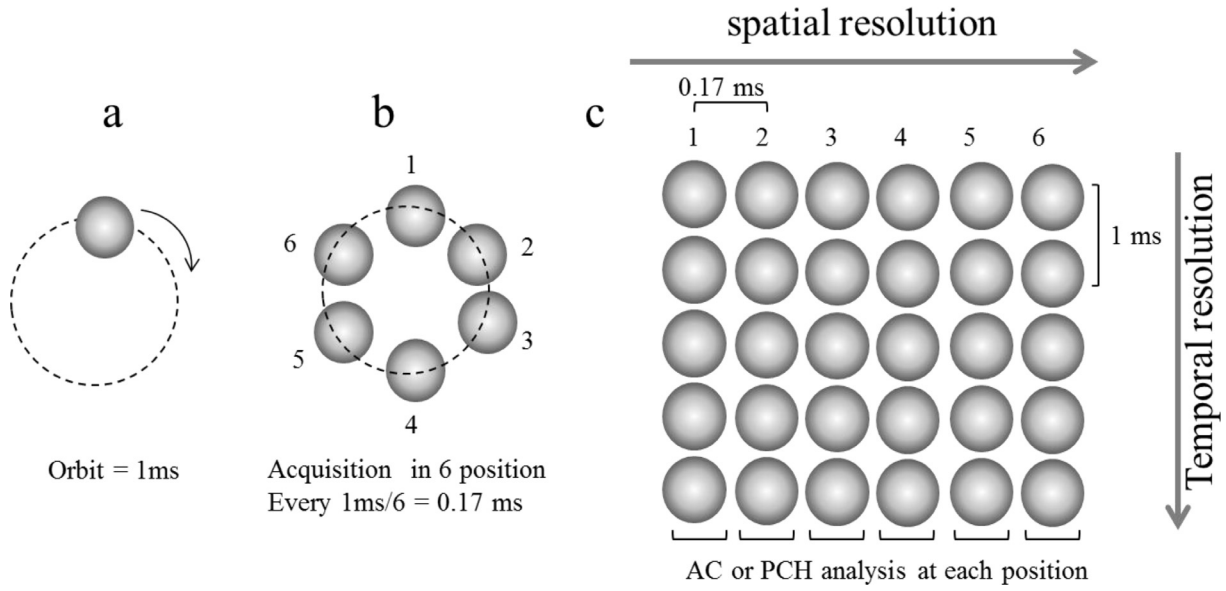

Fig. 4. Circular scanning FCS: data acquisition and analysis. (a) The small illumination volume (gray sphere) is moved in a circular orbit in a given time (1ms in this diagram). (b) During this time data can be obtained from different locations (1–6 in this example). (c) For the analysis, the data are organized in a x/y matrix (carpet) where each vertical set of data (taken every 1 ms) will characterize the fluctuations in any given position.

If the scanner performs a circular orbit of radius A with angular frequency ω around a center, Eq. (2) splits into the product of two functions: the autocorrelation function for the circular scanning (S(τ)) and the autocorrelation without scanning, equivalent to the autocorrelation function due to diffusion (G(τ)). Thus, assuming a three-dimensional Gaussian excitation profile with a radial waist w_0 and axial waist w_z.

$$S(\tau) = \exp\left(\frac{4A^2(1-\cos(\omega\tau))}{\left(1+\frac{4D\tau}{w_0^2}\right)w_0^2}\right) \tag{3}$$

$$G(\tau) = \frac{\gamma}{N}\left(1+\frac{4D\tau}{w_0^2}\right)^{-1}\left(1+\frac{4D\tau}{w_z^2}\right)^{-1/2} \tag{4}$$

Replacing Eqs. (3) and (4) into Eq. (2), one can fit the autocorrelation functions from circular-scan experiments to extract the diffusion coefficient, D_{coef}, of the particle using the geometrical factors that describe the beam profile (w0 and wz), the radius of the orbit A and the angular frequency ω of circular scanning.

2. Instrumentation

The instruments used in the applications discussed above were homebuilt at the Laboratory for Fluorescence Dynamics and the detailed description has been published [23,29]. (We note, though, that several commercially microscope systems – for example from Zeiss and Olympus, are also capable of performing scanning FCS). We will briefly describe the general instrumentation here and the details will be given in the applications. The instrument used was a custom made two-photon excitation scanning fluorescence microscope. The system was mounted on a commercial inverted microscope coupled to a mode-locked titanium-sapphire laser as the excitation light source. The laser beam was directed into the microscope by a set of galvonometric scanning mirrors used for circular scanning of the beam. A dichroic mirror reflects the excitation light into the objective and for detection of the emitted light, either one or two photomultipliers were used in the photon-counting mode. Optical filters can be placed before the photomultiplier according to the application and normally a BG39 optical filter (broad band-pass filter with a pass band from 350 nm to 600 nm) is placed for efficient suppression of IR excitation light. The data are collected and stored in a PC [23].

For circular scanning the two (x and y) galvomotor-driven scanning mirrors are driven by two identical sine waves with a 90° phase-shift. The laser beam moves in a circular path at the desired frequency and with a radius controlled by the amplitude and frequency of the sine wave. The center of the circular path can be changed by changing the DC offset values of the output waves. The data acquisition process begins with a fast raster scan over the entire sample range. Afterwards, by clicking on the image the user defines the starting point for the circular scanning in a clockwise direction. Then the laser beam scans in a circular orbit and the fluorescence intensity is collected at high frequency (64,000 Hz) as the laser moves (with the radius already defined) in circles around the chosen location [23,29,36].

3. General experimental considerations and controls

3.1. Labeling and the appropriate dye

The use of fluorescence techniques requires labeling the molecules of interest unless the molecule naturally fluoresces. The appropriate methodologies for labeling will be determined by the questions to be answered and this step can be crucial for data interpretation. For FCS it is particularly important that the fluorophore have a high intrinsic brightness, meaning a high extinction coefficient and a good quantum yield. The reason for this requirement is that the FCS method can usually be implemented only at low fluorophore concentrations, typically less than 0.01 mM (although exceptions exist). The reason for this restriction is that larger concentrations will not give rise to significant fluctuations in the signal. For example, the autocorrelation curves for Rhodamine 110 at various concentrations are shown in Fig. 5 [33]. As one can see these curves get progressively smaller as the concentration of fluorophore increases.

In FCS, three parameters are measured in the very small volume associated with the PSF, namely, number of particles, brightness and D_{coef}. Unspecific aggregation, homo-energy transfer (homo-

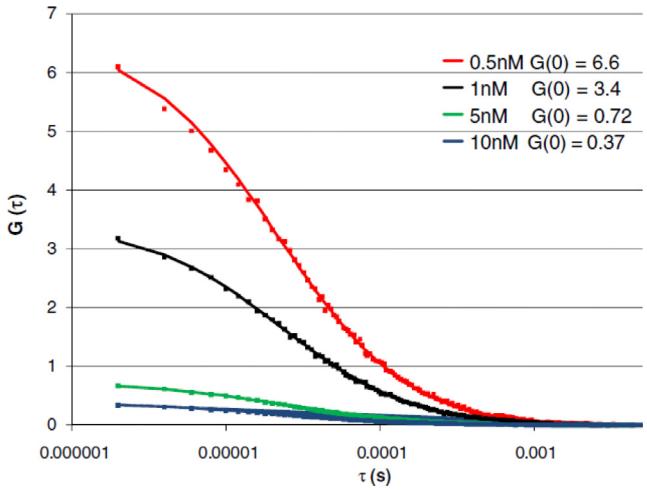

Fig. 5. Autocorrelation curves for Rhodamine solutions at different concentrations (from [33]).

FRET) and self-quenching will seriously alter these three parameters. If the studies involve elucidating the oligomeric state of a protein, for example, it is necessary that all subunits be labeled uniformally and that the fluorescence properties of the dye (e.g., quantum yield) are independent of the state of association [37,38]. Unspecific stickiness (especially when working with proteins in solution) of the sample to the coverslip will strongly confuse results on particle number.

3.1.1. Fluorescent antibodies

One of the early methods utilized for introducing fluorescence into a biological system was to label an antibody with a covalently attached probe, usually by coupling to a lysine or cysteine residue. Texts which discuss the chemistry of protein reactive groups and diverse labeling reagents used for protein conjugation are available [39,40]. Nowadays, researchers commonly buy antibodies already labeled with a probe. Although fluorescein- or rhodamine-based probes are available, antibodies labeled with more photostable fluorophores, such as the Alexa, Dylight or the Atto series of probes, are also available [24]. Characterization of the functional properties of the labeled antibody is also important. Often, the fluorescent labels are on secondary antibodies (i.e., an antibody that recognizes the primary antibody).

3.1.2. Fluorescent proteins

One of the most popular protocols to label proteins *in vivo* is by using molecular biological methods, in particular using Fluorescent Protein (FP) technology. New FPs are being reported almost every month and deciding which particular variant is best for your application can be a daunting task. A recent comprehensive review of the field was edited by Richard N. Day and Michael W. Davidson [41] although we also urge the reader to scan the latest literature and, if possible, to discuss the particular problem with experts before embarking on the time- and money-consuming business surrounding the required molecular biology. Another consideration when choosing an FP is the instrumentation available, for example, one or two-photon sources, since the excitation wavelengths available will certainly limit which FPs can be utilized. Genetic labeling can guarantee that all synthesized proteins have one GFP, however, over expression of the molecules can be a problem since FCS requires only a few particles. Therefore, delicate control of the expression level may be necessary. One should also take into account the endogenous levels of the target protein's expression. It is also important to consider that, although a good labeling strategy, GFP has a molecular weight of ~27 kD, and thus may interfere with measurements of diffusion coefficients of small proteins, i.e., the measured diffusion coefficient will correspond to the entire protein complex. We should note that most often EGFP (Enhanced Green Fluorescent Protein) is used instead of the original GFP. The EGFP contains a mutation which shifts the absorption maximum closer to 488 nm, the most often used output of the Argon-Ion laser popular in fluorescence microscopy and Fluorescence Activated Cell Sorting. Hence EGFP gives a larger signal, upon 488 nm excitation, than GFP – not because of any increase in intrinsic quantum yield but simply due to the shift in the absorption spectrum [42,43]. Also, some fluorescent proteins, including GFP, have been reported to form dimers at high concentrations [44], and those interested in utilizing FPs should consider this fact before choosing the FP for their experiments. Characterization of Förster resonance energy transfer in a botulinum 17551404876800neurotoxin protease assay, however, determined that the dissociation constant for wildtype GFP is in the range of 100 μM which may not be strong enough to influence many applications [45]. But each case should be considered separately. Many laboratories now utilize FPs containing the A206K mutation which disrupts oligomerization [46].

3.1.3. Biomolecular fluorescence complementation

A variation on genetically encoding FPs with target proteins is the biomolecular fluorescence complementation (BiFC) method. The BiFC method involves the attachment of nonfluorescent N- and C-termini of an FP, typically split between β-sheets 7 and 8, to the target proteins thought to interact. Upon association, if the three-dimensional properties of the complex permit, the FP halves can come together, promoting refolding of the two half into one intact FP and maturation of the fluorescent moiety, and hence producing fluorescence indicating association of the target proteins (reviewed in [14]).

3.1.4. Halo-Tags

Another labeling method utilizing genetic manipulation is the Halo Tag approach [14]. In this approach, the target protein is recombinantly fused with a mutated form of bacterial haloalkane dehalogenase. Reaction of this mutant dehalogenase with an appropriate halogenated aliphatic substrate, covalently attached to a fluorophore, will result in the covalent linkage of the fluorescent probe to the halogenase and thus the protein of interest. Hence, different fluorophores can be attached to the target protein. Since the dehalogenase is a bacterial enzyme, the labeling is specific and cross-reaction with mammalian proteins is eliminated. This method is suitable for cell surface proteins, such as receptors, which are accessible to the fluorescent substrate. Of course, the same considerations regarding the fusion of the dehalogenase and target protein genes mentioned in the section on FP constructs, also apply for the HaloTag approach. The SNAP-tag and FlAsH methods have also been used to introduce fluorescent probes *in vivo* and have been reviewed [14].

3.2. Concentration range and crowdedness

In FCS measurements, the concentration used is much lower than that required in most other techniques. Normally, FCS works best with concentrations in the nanomolar range, i.e. from 1 to 6 molecules in the excitation volume. In practical terms, this condition means FCS is most suitable to study equilibrium with dissociation constants in the nanomolar range or below. Inside the cells, the molecules are typically more concentrated than the nanomolar range, hence one should expect small values of G(0) and a long acquisition time (at low power) is required, as well as increasing the number of measurement, to insure the statistical significance of the data.

3.3. Autofluorescence

Phenol red is a major source of autofluorescence and should be removed from imaging medium. Cellular sources of auto fluorescence include, but are not limited to, flavins and flavoproteins (at 500–600 nm), reduced pyridine nucleotides (at 400–500 nm), and aromatic amino acids (although these amino acids, which absorb only in the UV region, are not a problem for one or two photon excitation). Dead, damaged, crowded, or otherwise stressed cells increase autofluorescence, indicating the importance of maintaining a healthy culture environment. Autofluorescence of biological material can be very strong at typical excitation and emission wavelengths and may depend on the cell type and its metabolic state. As a general observation two-photon excitation will minimize the auto-fluorescence excitation compared to one photon excitation, however control experiments for autofluorescence must be always done before starting any FCS experiment. Simple imaging of labeled and unlabeled cells, under the same experimental conditions of temperature, pH, growing time and especially laser power, will show if it is possible to discriminate the signal of the protein of interest from the background.

4. Selected applications

In this section we present applications using csFCS for two different biological problems. We selected these two applications since they required different experimental setups, controls and analysis.

4.1. Ribosomal structure and the power of PCH analysis for in vivo studies [24]

Saccharomyces cerevisiae ribosomes are composed of two subunits (60S and 40S). In an active ribosome, in the 60S unit, a structure called the stalk contains, on average, five distinct proteins,

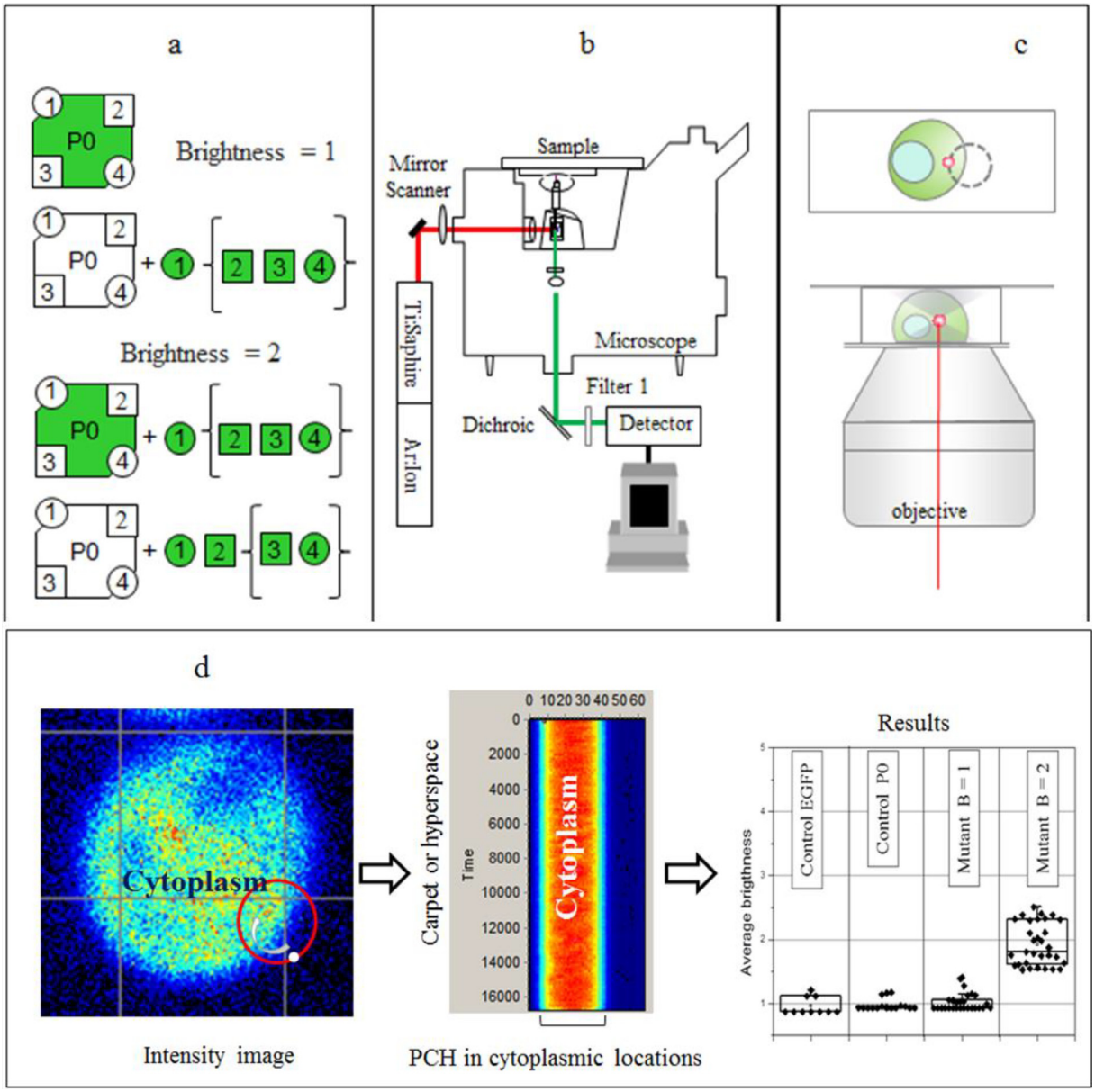

Fig. 6. *In vivo* studies of *S. cerevisiae* ribosomal structure by circular FCS and PCH analysis. (a) Experimental strategy (b) Instrumentation (c) sample preparation (d) data analysis and results [24].

namely P0 and four acidic proteins, P1α, P1β, P2α, and P2β. Each ribosome contains only one copy of P0, but the distribution of the acidic proteins among the ribosome population may differ. Some hypotheses state that cellular pattern of expressed proteins may be determined by the distribution of the stalk proteins among the ribosome population. To assess ribosomal heterogeneity *in vivo*, two-photon circular scanning FCS and PCH analysis was used [24]. The results showed that csFCS and PCH analysis could distinguish *in vivo* ribosomes with one or two labeled components, demonstrating that a combination of the acidic proteins and P0 exist *in vivo*.

4.1.1. Experimental approach (Fig. 6a)

The experimental strategy consisted of expressing *in vivo* different combinations of EGFP-labeled-proteins leading to ribosomes labeled with one or two EGFPs. EGFP- proteins (P0 or any of the four acidic proteins) were expressed in knockout strains and the technical challenge consisted in distinguishing brightness of 1

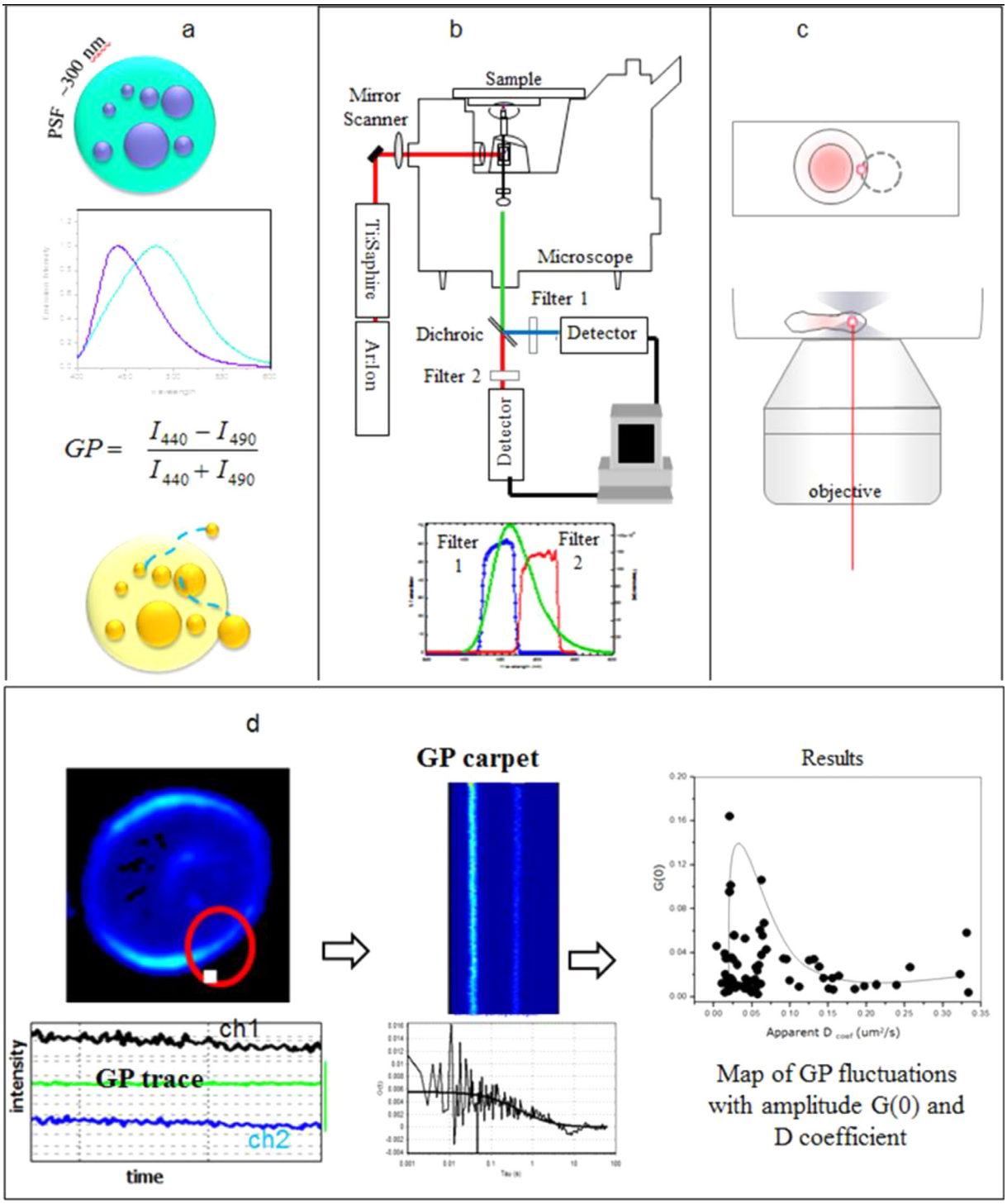

Fig. 7. Detection of lipid domains *in vivo* by mixing scanning FCS and Laurdan GP. (a) Experimental strategy (b) instrumental setup (c) sample preparation (d) data analysis and results [25].

(one molecule of EGFP) or 2 (two molecules of EGFP) in live cells using csFCS and PCH analysis.

4.1.2. Instrumental setup: (Fig. 6b)

The instrument used was a homebuilt two-photon excitation scanning fluorescence microscope with one channel detection. The excitation source was a Mode-locked titanium-sapphire laser with 80-MHz, 100-fs pulse width (Tsunami; Spectra-Physics, Mountain View, CA) tuned to 920 nm. Movement of the laser beam in a circular orbit was performed by two (x-y) galvanoscanner mirrors (Model 6350; Cambridge Technology, Watertown, MA). The emitted light was detected using a photomultiplier tube (Hamamatsu R7400P, Hamamatsu City, Japan) in photon counting mode through a BG39 optical filter (Chroma Technologies, Brattleboro, VT) for suppression of IR excitation light. The objective used was an Olympus 60× (1.2 N.A.) water immersion.

4.1.3. Sample preparation

S. cerevisiae strain (BJ5458) was used to generate 26 EGFP mutants (Fig. 6c). Yeast at the same growing stage (absorbance at 600 nm was 0.5 OD at 25 °C) were immobilized in 2% agarose (Fig. 6c) and measured at 25 °C to minimize growing.

4.1.4. Troubleshooting

Two controls were measured. (1) control for autofluorescence: before transfection, several *S. cerevisiae* strains were tested. The chosen strain (BJ5458) presented low autofluorescence at the working wavelength (two photon 920 nm) allowing a high signal/noise ratio for EGFP. (2) Control for daily laser power variations: together with the experimental sample two controls were measured to account for brightness = 1: control, yeast expressing free EGFP in the cytosol and yeast expressing only P0-EGFP.

4.1.5. Data acquisition and analysis

(Fig. 6d). The data acquisition frequency was set at 64 kHz, with a 1-ms orbit period and radius of 1.52 μm. The pixel size in the orbit was 0.148 μm. For data analysis, the intensity data were transformed into a x-y representation (carpet) (Fig. 6d) and the 64 locations registered. From the carpet, 4–5 locations inside the cytosol were analyzed by PCH. Data results were represented in a box chart where control samples were used to normalize the brightness of the mutants having brightness of 1 or 2.

4.2. Lipid domains in vivo: mixing scanning FCS and Laurdan GP. [25]

The heterogeneity of cellular membranes is understood these days to include the existence of small highly packed and dynamic structures (10–200 nm), often denominated as rafts. Scanning FCS (high temporal resolution) and Laurdan GP (highly sensitive to membrane packing) were combined in this study to characterize *in vivo* membrane heterogeneity. This combined methodology was successfully used to characterize Laurdan GP fluctuations in biological membranes that could be explained by the existence of tightly packed micro-domains moving in a more fluid background phase with a size range comparable to the one proposed for lipid rafts.

4.2.1. Experimental approach (Fig. 7a)

The aim of this application was to detect membrane domains smaller than the PSF (diameter of ~300 nm) (Fig. 7a). The spectra of Laurdan in the erythrocyte membrane would be centered on 440 nm or 490 nm depending if the membrane domain (where Laurdan is immersed) is well packed (~440 nm) or more fluid (~490 nm), respectively. The autocorrelation analysis of each channel gives information about Laurdan molecules moving in and out of the illumination volume, but could not report changes in lipid packing at the nanoscale range. The experimental challenge was to detect fluctuations in Laurdan GP, which could be related to fluctuation of domains with different packing in the membrane of erythrocytes and CHO cells in culture.

4.2.2. Instrumental setup: (Fig. 7b)

A two-photon excitation scanning fluorescence microscope with a two-channel detection system was used. The excitation source was a Mode-locked titanium sapphire laser (Mira 900; Coherent) pumped by a frequency-doubled Nd: Vanadate laser (Verdi, Coherent) set to 780 nm. The laser beam was circularly scanned using two galvanoscanner mirrors (Cambridge Technology).

Objective: LD Achroplan 60X long working distance water objective 1.2NA (Olympus America Inc.) In the emission path, a dichroic beam splitter (Chroma Technology 470DCXR-BS), a broad band-pass filter (BG39 filter, Chroma Technology, Brattleboro, VT) and two interference filters Ealing 440 ± 50 nm (Filter 1 Fig. 7b) and Ealing 490 ± 50 nm (Filter 2 Fig. 7b) were used for simultaneously detection by two miniature photomultipliers (R5600-P, Hamamatsu, Bridgewater, NJ).

4.2.3. Sample preparation

Erythrocytes were isolated by centrifugation and suspended to the original hematocrit and kept at 37 °C. Samples were diluted to a hematocrit of 0.2% in PBS containing 0.4 μM Laurdan, incubated 15 min and observed under the microscope at 37 °C.

4.2.4. Troubleshooting: four controls were tested

(1) Control for fluctuations: Giant Unilamellar vesicles (GUVs) made of POPC labeled with Laurdan and measured at 37 °C. At this temperature POPC will be in a liquid state (Tm is -2°C) and csFCS showed no autocorrelation in the GP signal. (2) Control for cell type. In a blood sample there are normally erythrocytes with disc shape and also echinocytes. Just the discoid cells were measured. (3) Control for cell aging: reported data were obtained from erythrocytes from blood from the day of withdrawing and the next day. The observation was that the data taken after day 3, showed mainly large domains. (4) Control for autofluorescence and survival of the cells: samples received from 0.5 to 1.5 mW of the excitation light.

4.2.5. Data acquisition and analysis

The data acquisition frequency was set at 64 kHz, with a 1-ms orbit period and radius of 1.52 μm. The pixel size in the orbit was 0.148 μm. Sixty-four data points, corresponding to 64 locations, were collected in each scanning orbit. For data analysis, the intensity data were transformed in a x-y representation (Fig. 7d) and the 64 locations registered. Locations corresponding to the membrane were analyzed by autocorrelation and two parameters were obtained: G(0) and Diffusion coefficient ($\mu m^2/s$). Results (Fig. 7d) were represented in a plot of G(0) versus Diffusion coefficient. These maps of domains proved to be similar to CHO cells and changed in distribution when cholesterol was removed [25].

Acknowledgements

Financial support: FONDECYT – Chile #1140454 (S.S.), FONDECYT – Chile #1080412 (G.G.) and Beca de Doctorado Conicyt (C.S.).

References

[1] A. Einstein, Über die von der molekularkinetischen Theorie der Wärme geforderte Bewegung von in ruhenden Flüssigkeiten suspendierten Teilchen, Ann. Phys. 322 (1905) 549–560.
[2] M. Smoluchowski, Zur kinetischen Theorie der Brownschen Molekularbewegung und der Suspensionen, Ann. Phys. 21 (1906) 756–780.

[3] T. Svedberg, K. Inouye, Eine neue Methode zur Prüfung der Gültigkeit des Boyle-Gay-Lussacschen, Z. Phys. Chem. 77U (1911) 145–191.
[4] E. Elson, D. Magde, Fluorescence correlation spectroscopy. Conceptual basis and theory, Biopolymers 13 (1974) 1–27.
[5] D. Magde, E.L. Elson, W.W. Webb, Fluorescence correlation spectroscopy. II. An experimental realization, Biopolymers 13 (1974) 29–61.
[6] B. Ehrenberg, R. Rigler, Rotational brownian motion and fluorescence intensity fluctuations, Chem. Phys. 4 (1974) 390–401.
[7] W. Denk, J.H. Strickler, W.W. Webb, 2-Photon laser scanning fluorescence microscopy, Science 248 (1990) 73–76.
[8] K.M. Berland, P.T.C. So, E. Gratton, 2-photon fluorescence correlation spectroscopy - method and application to the intracellular environment, Biophys. J. 68 (1995) 694–701.
[9] E.L. Elson, Quick tour of fluorescence correlation spectroscopy from its inception, J. Biomed. Opt. 9 (2004) 857–864.
[10] E.L. Elson, Fluorescence correlation spectroscopy: past, present, future, Biophys. J. 101 (2011) 2855–2870.
[11] E.L. Elson, 40 years of FCS: how it all began, Method Enzymol. 518 (2013) 1–10.
[12] M. Weissman, H. Schindler, G. Feher, Determination of molecular-weights by fluctuation spectroscopy – application to DNA, Proc. Natl. Acad. Sci. USA 73 (1976) 2776–2780.
[13] N.O. Petersen, Scanning fluorescence correlation spectroscopy. 1. Theory and simulation of aggregation measurements, Biophys. J. 49 (1986) 809–815.
[14] D.M. Jameson, N.G. James, J.P. Albanesi, Fluorescence fluctuation spectroscopy approaches to the study of receptors in live cells,, Fluor. Fluctuat. Spectrosc. (Ffs) Pt B 519 (2013) 87–113.
[15] D.M. Jameson, Introduction to Fluorescence, Taylor and Francis, New York, NY, 2014.
[16] Y. Chen, J.D. Muller, K.M. Berland, E. Gratton, Fluorescence fluctuation spectroscopy, Methods 19 (1999) 234–252.
[17] J.D. Muller, Y. Chen, E. Gratton, Resolving heterogeneity on the single molecular level with the photon-counting histogram, Biophys. J. 78 (2000) 474–486.
[18] D.E. Koppel, F. Morgan, A.E. Cowan, J.H. Carson, Scanning concentration correlation spectroscopy using the confocal laser microscope, Biophys. J. 66 (1994) 502–507.
[19] K.M. Berland, P.T.C. So, Y. Chen, W.W. Mantulin, E. Gratton, Scanning two-photon fluctuation correlation spectroscopy: Particle counting measurements for detection of molecular aggregation, Biophys. J. 71 (1996) 410–420.
[20] J.P. Skinner, Y. Chen, J.D. Muller, Position-sensitive scanning fluorescence correlation spectroscopy, Biophys. J. 89 (2005) 1288–1301.
[21] J. Mutze, T. Ohrt, P. Schwille, Fluorescence correlation spectroscopy in vivo, Laser Photon. Rev. 5 (2011) 52–67.
[22] Q.Q. Ruan, M.A. Cheng, M. Levi, E. Gratton, W.W. Mantulin, Spatial-temporal studies of membrane dynamics: Scanning fluorescence correlation spectroscopy (SFCS), Biophys. J. 87 (2004) 1260–1267.
[23] Q.Q. Ruan, Y. Chen, E. Gratton, M. Glaser, W.W. Mantulin, Cellular characterization of adenylate kinase and its isoform: two-photon excitation fluorescence imaging and fluorescence correlation spectroscopy, Biophys. J. 83 (2002) 3177–3187.
[24] A. Garcia-Marcos, S.A. Sanchez, P. Parada, J. Eid, D.M. Jameson, M. Remacha, E. Gratton, J.P.G. Ballesta, Yeast ribosomal stalk heterogeneity in vivo shown by two-photon FCS and molecular brightness analysis, Biophys. J. 94 (2008) 2884–2890.
[25] S.A. Sanchez, M.A. Tricerri, E. Gratton, Laurdan generalized polarization fluctuations measures membrane packing micro-heterogeneity in vivo, Proc. Natl. Acad. Sci. USA 109 (2012) 7314–7319.
[26] A. Celli, E. Gratton, Dynamics of lipid domain formation: Fluctuation analysis, Biochim. Biophys. Acta Biomembr. 1798 (2010) 1368–1376.
[27] A. Celli, S. Beretta, E. Gratton, Phase fluctuations on the micron-submicron scale in GUVs composed of a binary lipid mixture, Biophys. J. 94 (2008) 104–116.
[28] J. Ries, S. Chiantia, P. Schwille, Accurate determination of membrane dynamics with line-scan FCS, Biophys. J. 96 (2009) 1999–2008.
[29] M.A. Digman, P. Sengupta, P.W. Wiseman, C.M. Brown, A.R. Horwitz, E. Gratton, Fluctuation correlation spectroscopy with a laser-scanning microscope: Exploiting the hidden time structure, Biophys. J. 88 (2005) L33–L36.
[30] P. Muller, P. Schwille, T. Weidemann, in: Y. Engelborghs, A.J.W.G. Visser (ed.), Fluorescence Spectroscopy and Microscopy: Methods and Protocols, Humana Press, 2014.
[31] M. Huertas de la Torre, R. Forni, G. Chirico, Brownian dynamics simulations of fluorescence fluctuation spectroscopy, Eur. Biophys. J. Biophys. Lett. 30 (2001) 129–139.
[32] F. Cardarelli, E. Gratton, In vivo imaging of single-molecule translocation through nuclear pore complexes by pair correlation functions, Plos One 5 (2010).
[33] D.M. Jameson, J.A. Ross, J.P. Albanesi, Fluorescence fluctuation spectroscopy: ushering in a new age of enlightenment for cellular dynamics, Biophys. Rev. 1 (2009) 105–118.
[34] P. Schwille, U. Haupts, S. Maiti, W.W. Webb, Molecular dynamics in living cells observed by fluorescence correlation spectroscopy with one- and two-photon excitation, Biophys. J. 77 (1999) 2251–2265.
[35] M.A. Digman, C.M. Brown, P. Sengupta, P.W. Wiseman, A.R. Horwitz, E. Gratton, Measuring fast dynamics in solutions and cells with a laser scanning microscope, Biophys. J. 89 (2005) 1317–1327.
[36] V. Levi, Q. Ruan, K. Kis-Petikova, E. Gratton, Scanning FCS, a novel method for three-dimensional particle tracking, Biochem. Soc. Trans. 31 (2003) 997–1000.
[37] S.A. Sanchez, J.E. Brunet, D.M. Jameson, R. Lagos, O. Monasterio, Tubulin equilibrium unfolding followed by time-resolved fluorescence and fluorescence correlation spectroscopy, Protein Sci. 13 (2004) 81–88.
[38] S.A. Sanchez, Y. Chen, J.D. Muller, E. Gratton, T.L. Hazlett, Solution and interface aggregation states of Crotalus atrox venom phospholipase A(2) by two-photon excitation fluorescence correlation spectroscopy, Biochem.-Us 40 (2001) 6903–6911.
[39] G.T. Hermanson, Bioconjugate Techniques, Academic Press, San Diego, CA, 1996.
[40] S.S. Wong, D.M. Jameson, Chemistry of Protein and Nucleic Acid Cross-Linking and Conjugation, Tayor and Francis, New York, NY, 2012.
[41] R.N. Day, M.W. Davidson, The Fluorescent Protein Revolution, CRC Press, New York, 2014.
[42] B.P. Cormack, R.H. Valdivia, S. Falkow, FACS-optimized mutants of the green fluorescent protein (GFP), Gene 173 (1996) 33–38.
[43] R. Heim, A.B. Cubitt, R.Y. Tsien, Improved green fluorescence, Nature 373 (1995) 663–664.
[44] L.M. Costantini, M. Fossati, M. Francolini, E.L. Snapp, Assessing the tendency of fluorescent proteins to oligomerize under physiologic conditions, Traffic 13 (2012) 643–649.
[45] J.A. Ross, M.A. Gilmore, D. Williams, K.R. Aoki, L.E. Steward, D.M. Jameson, Characterization of forster resonance energy transfer in a botulinum neurotoxin protease assay, Anal. Biochem. 413 (2011) 43–49.
[46] D. von Stetten, M. Noirclerc-Savoye, J. Goedhart, T.W.J. Gadella, A. Royant, Structure of a fluorescent protein from Aequorea victoria bearing the obligate-monomer mutation A206K, Acta Crystallogr. F 68 (2012) 878–882.